Adaptive Robotic HVAC Duct Cleaner Using Rubber-Traction Omniwheels and W-Shaped Pantograph Design

Ansh Singh[1] and Reetu Jain[2]

[1] Class of 2025, Oberoi International OGC.
dipti.vaishnav@gmail.com
[2] Mentor, On My Own Technology Pvt. Ltd., Lokhandwala, Oshiwara, Mumbai, India.
reetu.jain@onmyowntechnology.com

Abstract. Heating, ventilation and air conditioning (HVAC) systems are essential in facilitating indoor air quality (IAQ) but often accumulate dust, allergens and other microbial contaminants that may have negative psychosocial effects on human health. Traditional duct-cleaning techniques like air whips, rotating brushes and steam cleaning systems can all be limited in their efficiency, and are often potentially dangerous to maintenance personnel. This research proposes a new Robotic cleaning system that comprises a W-shaped pantograph, that has eight omniwheels, designed to enhance maneuverability and adaptability in the duct-cleaning process. The system is capable of vertical climbing and lateral movement through controlled spring compressive forces, that optimize friction against duct walls. It is operational in both circular and rectangular ducts, and it can function in ducts of ranges between 11 and 22 cm diameter. Structural simulations performed in ANSYS revealed peak von Mises stresses of 1.32×10^5 Pa, significantly below the yield thresholds of PLA (4.4×10^7 Pa) and ABS (6.0×10^7 Pa), confirming structural safety with a safety factor greater than 10.Furthermore, the design to include spring assisted axial movement provides enhanced maneuverability and reduces energy expenditure to navigate to compressed regions. The conclusions of this work demonstrates a feasible solution to performing HVAC duct cleaning in a safer, efficient and cost-effective manner than existing methods.

Keywords: Indoor Air Quality (IAQ), HVAC Systems, Robotic Duct Cleaning, W-Shaped Pantograph, Omniwheels, ANSYS Simulation, Structural Safety, Energy Efficiency.

I. INTRODUCTION

Heating, ventilation, and air conditioning (HVAC) systems are critical to maintaining indoor air quality (IAQ) and thermal comfort indoors in a residential, commercial, and industrial space. Dust, allergens, and microbial contaminants can accumulate in ducts over time causing health issues in a variety of ways.

For instance, in an average six-bedroom household, there can be an accumulation of as much as 13.6–18.1 kgs of dust in HVAC ducts, which combines with an increase in the incidences of respiratory disease by as much as 25–30% (i.e., asthma, chronic obstructive pulmonary disease (COPD), allergies). According to the American Lung Association, poor IAQ associated with contaminated HVAC systems accounts for approximately 3.8 million deaths per year globally from urban air pollution.

In addition, moisture-saturated ducts compound the risk for health problems by promoting the growth of bacteria, fungi, and pollen. The microbial activity produces bioaerosols and volatile organic compounds (VOCs) that, even in low concentrations, can irritate the eyes and throat and cause serious health problems leading to conditions of the liver and kidneys at higher exposure concentrations.

Conventional cleaning technologies including rotating brushes, compressed air whips and steam cleaning have had great success, but newer HVAC systems require much more adaptability than these tools can offer. Rotating brushes can be great at removing stubborn debris inside of ductwork - but they are not usable with fragile ductwork and impractical for large commercial applications that demand compact, highly mobile cleaning options. Compressed air cleaning can remove loose dust from complicated duct networks - but does so at the cost of removing contaminants that are firmly adhered. Steam cleaning also adds additional variables like moisture retention in ducts and operator safety.

To address cleaning technologies that need more versatility, my proposed solution is a new robotic cleaning system that has a W-shaped pantograph and eight omniwheels. The installation is versatile for usable ducts with a diameter ranging from 11-22 cm, and usable for both circular and rectangular shapes, elbows and T-joints. The omniwheel design allows for much better mobility by allowing vertical climbing, lateral shifting, and turning and/or rolling around the walls of the duct that standard cleaning methodologies cannot support. The structural simulations also show that the design can be used with a compressive force of about 15 kg with limited deformation, allowing operational effectiveness and operational stability.

By combining adaptability, mobility, and safety, the proposed robotic system advances beyond existing HVAC cleaning approaches, offering a reliable and effective solution for improving IAQ in residential and commercial environments.

II. LITERATURE REVIEW

Momma et al. [1] studied the accumulation of grease in kitchen ventilation ducts, a danger for fire and maintenance concerns, and proposed a cleaning system using a multistage planetary gear mechanism which could scrub the square duct sidewalls with a brushing velocity of over 60 mm/s. Their prototype provided a 91% cleaning effectiveness, which was significantly higher than the 80% effectiveness threshold established for duct cleaning. Although presented with promising results, there were still significant issues with brush contamination, energy loss from wire–wall contact, and lack of general speed control, which suggest that prototype improvements are still needed.

Yan et al. [2] researched impurity accumulation in HVAC pipelines which is both a concern for safety and efficient operation, and developed an autonomous cleaning robot in the form of a spiral combined with a water jet cleaning system. Through optimization in experiments it was systematically determined that a nozzle distance of 25 mm, jet angle of 15°, and pressure of 30 MPa produced maximum shear force from the water for cleaning. However, despite good shower size, shape, and velocity of water for cleaning in experiments, the cleaning system was less effective at higher angles (30°, 45°) and performed poorly with varying pipe geometries, which indicates the need for improved adaptability.

Husainy et al. [3] investigated biological contamination in heating, ventilation and air conditioning (HVAC) ducts and the associated health exposure risk to maintenance workers. The researchers designed a multi-function rover robot equipped with rotating brushes, microscopic camera, and Eulerian Video Magnification (EVM) for real-time contamination detection and cleaning execution. The robotic system adapted to the varying duct geometries (e.g., rectangular or circular) and operations reduced exposure and risk for the maintenance worker. The research concluded that the system was a mobile and adaptable tool for contamination surveillance and detection/cleaning; while the overall results were promising, the system's robustness and scalability and autonomous operations under local duct conditions were yet to be demonstrated.

Aureliano et al. [4] identified robots as replacements for hazardous manual cleaning of air-conditioning duct systems. The robot was designed with rotating brushes, microscopic camera, and EVM to observe and remove microbial contaminations. The researchers successfully improved safety/operator risk, flexibility, and adaptation with the robotic technology, but highlighted important limitations in scaling the technology for larger air conditioning systems and the requirement to focus on optimizing the autonomous operation of the robotic system.

Bubanja et al. [5] studied dust and microbial accumulation in HVAC ducts, and built a semi-autonomous robotic cleaner with replaceable brush attachments, rechargeable batteries, ultrasonic sensors, and an HD camera. The robot showed successful cleaning and inspection capabilities for rectangular and round ducts, and works with both wireless and semi-autonomous control options, although their study noted further research on both brush extensions and attachments still continued to be relevant for experience, performance and understanding.

Seo et al. [6] addressed the challenge of real-time navigation across complicated duct geometries, developing a three-legged robot with an ultra-wideband (UWB) communication module and using a gradient descent–based trilateration algorithm for position estimation. The robot successfully identified T-ducts 95% of the time, except when there was error in distance estimation when staying near metallic ducts, it was also vulnerable to light interference, and rectangular ducts hindered the robot's movement.

Tanise et al. [7] investigated the use of a peristaltic crawling robot powered by artificial muscles to perform cleaning of narrow and curved residential ventilation ducts. Their optimized system achieved cleaning performance of 97.4%. The study noted, however, that the system did not achieve its target cleaning performance of 99.8%, and additional work is needed to improve scraping efficiency and to reach a broader validation over different HVAC systems.

Shao et al. [8] conducted a review of in pipe cleaning robots and categorized robots by locomotion type (wheeled, caterpillar, PIG), by sensor systems (ultrasonic, vision), and by cleaning methods (water jet, brushes). Their review asserted that there is no existing robotic system capable of adapting to the entire range of pipe shapes and environments, and they reiterated that developing automated cleaning methods remains a challenge.

Bulgakov et al. [9] detailed a telerobotic cleaning design for HVAC ductwork which utilizes a combination of air jets, chemical sprays and ultraviolet LEDs for microbial dose reduction. A fuzzy logic position control scheme was implemented to improve maneuverability. The system performed successful coverage of an area up to a value of 2827.43 m^2. Limitations of the system included tethering of the machine to the chemical supply which hampered mobility, as well as consideration of the chemicals used for disinfecting in sensitive environments such as a hospital.

Cleaning difficulties with central AC ventilation systems in China were addressed by Li et al. [10]. The PCV-11 robot was created with a spring-type mechanism to navigate both horizontal and vertical ducts that could vary in diameter between 300-600 mm. The robot was able to navigate sections with elbows or bends while also maintaining stability while cleaning. The robot utilized a tethered communication cable instead of a wireless option, and therefore, lacked much flexibility in use.

Tavakoli et al. [11] invented a pole-climbing robot (PCR) for the non-destructive testing (NDT) of industrial pipes. Their design included four degrees of freedom, V-grippers and accelerometers to monitor grip and orientation. The robot performed as required while testing industrial pipes of 219 mm in diameter but experienced gripper misalignment issues, requiring manual correction and spotlighting the need for the robot to have autonomous correction abilities.

Wang et al. [12] created an autonomous duct-cleaning robot to resolve problems related to indoor air pollution with dirty ducts contributing to sick building syndrome (SBS). Their prototype included a guided-allocation device and adjustable wheels to assist with movement. The robot had successful and effective cleaning in controlled conditions, but the system did not possess overall autonomy and required testing once further developed outside of controlled conditions.

Virk et al. [13] explored robotic cleaning options for dirty and hazardous environments such as HVAC ducts. Their modular robot with vacuum suction grippers was able to operate on surfaces (e.g., floor-to-wall, and wall-to-ceiling). While the robot was undoubtedly versatile, its size and power efficiency remained problematic for the design overall.

Zhang et al. [14] developed "Sky Cleaner," a climbing robot designed to clean vertical glass facades. The robot boasted a vacuum pad, XY piston drive, and several sensors in order to clean effectively and efficiently over curved and flat surfaces. Even with advancements, the cleaner in its given design faced issues such as battery life, motor noise, and bulk in its commercial application, demonstrating opportunities for further miniaturization and optimization in the design.

III. Methodology

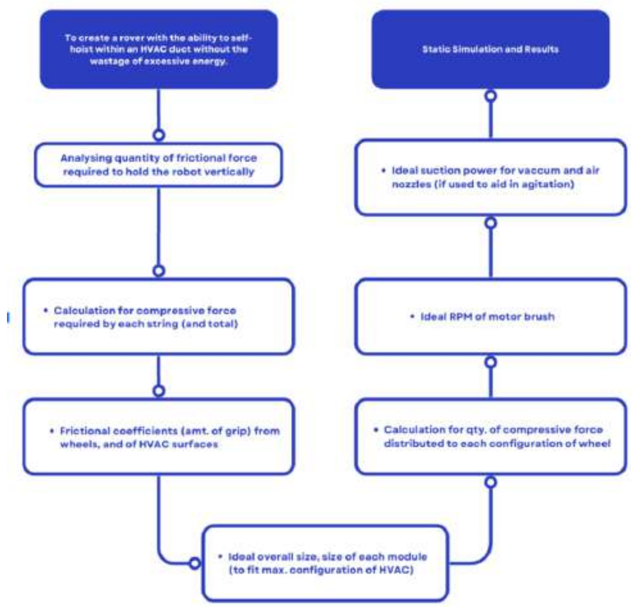

Fig. 1. Flowchart of Methodology

Figure 1 presents the overall methodology of the research, starting with the problem statement and ending with the idea of static simulation analysis. The methodology began by computing the frictional force needed to lift the weight of the robot up-and-down in HVAC ducts to support it in a vertical position. This led to a calculation of the required compressive force per spring that would be needed to generate an amount of traction for self-hoisting. The study measured the frictional coefficients of HVAC surfaces, either clean or dusty, in measurements of grip achievable with omniwheels.

Using the target duct dimensions of 11cm–22cm. the overall geometry of the W-shaped pantograph and its modular assemblies were defined. The calculations identified how large the compressive forces would work across the wheels of the robot, allowing for a motor selection to be made, along with their required power output. For the cleaning mechanism, the least amount of running speeds of the motorized brushes, and suction power of the vacuum and air nozzles, based on levels of dust collected, were also calculated to save on energy running cost.

Design and Modeling of the W-Shaped Spring Structure

The robotic subsystem was developed around a novel W-shaped pantograph frame modeled in SolidWorks. The pantograph consists of rigid arms connected through rotational joints, enabling symmetrical expansion and compression under the preload of centrally mounted coil springs. This configuration ensures structural stability by minimizing torsional flex during expansion.

At the terminal ends of each pantograph arm, omniwheels were mounted to maintain continuous contact with the duct walls. The spring system was designed to balance the required normal force with allowable deflection limits, preventing over-compression while ensuring reliable traction. Output force–displacement behavior for different spring configurations was optimized using motion simulations in SolidWorks and validated in ANSYS.

Co-Design and Integration of Wheel–Spring Mechanism

The omniwheel and spring mechanisms were co-designed to ensure synchronized operation. Each omniwheel hub is coupled with a spring-loaded channel that exerts normal force perpendicular to duct surfaces, thereby adapting to uneven geometries.

The wheels were fabricated with PLA cores for rigidity and TPU (Thermoplastic Polyurethane) treads for compliance and grip. This material combination provides sufficient stiffness for torque transfer while absorbing surface irregularities, preventing damage to thin aluminum or composite ducts. Springs were selected according to Hooke's law, calibrated to operate within the calculated range of normal forces. The system achieves a traction margin of 15–20% above the theoretical minimum, enabling stable vertical climbing and lateral traversing in both circular and rectangular ducts.

Simulation and Analysis

The SolidWorks assembly was imported into ANSYS for multiphysics analysis across three operational scenarios:

1. **Static Support:** The robot was held upright to test whether spring compression alone could sustain structural weights between 5–10 kg. The maximum simulated von Mises stress was 1.32×10^5 Pa, well below the yield limits of PLA (4.4×10^7 Pa) and ABS (6.0×10^7 Pa), confirming safe design margins.

2. **Vertical Motion Initiation:** Acceleration and deceleration forces during climbing were simulated. Results confirmed stable wheel traction with negligible deformation (1.03×10^{-13} m), indicating near-rigid response and no slippage under initial motion.
3. **Dynamic Cleaning Operation:** Simulations involving vibrations, duct junction impacts, and rotational transitions demonstrated that the structure consistently maintained a safety factor above 10. Stress concentrations remained well below material limits, while TPU components effectively absorbed vibration loads, enhancing operational stability and durability.

Force Parameter Definitions

Frictional Force: In a vertical duct, the robot's weight is expressed as $W = mg$, where m is the mass (kg) and $g = 9.81\,\mathrm{ms}^{-2}$ is the gravitational acceleration acting directly downward. To avoid slipping, the total frictional force F_f at the contact interfaces must at least equal this weight:

$$F_f \geq W \tag{1}$$

$$F_f \geq mg \tag{2}$$

According to Coulomb's law of friction:

$$F_f = \mu N = mg \tag{3}$$

where μ is the coefficient of static friction between the robot's wheel and duct wall, and N is the net normal force pressing the robot against the wall, due to the spring force applied from each of the rover's wheels.

Compressive Force Distribution: Fine dust deposited on the surface can reduce μ by up to 50%. Hence, the minimal required normal force is given by:

$$N \geq mg \tag{4}$$

Isolating N (net normal force):

$$N \geq mgs \tag{5}$$

If the robot employs n spring-loaded legs, where each wheel equally shares the load, each wheel must generate:

$$N_{\text{each}} = \frac{N}{n} \tag{6}$$

Since $N_{\text{each}} \cdot n \geq N$:

$$N_{\text{each}} \geq \frac{mgs}{n} \tag{7}$$

Spring Force and Preload Calculation: To start off with the height adjuster, coil springs are fixed with each leg to allow expansion and compression.

According to Hooke's Law, the force exerted by a spring compressed or extended by displacement x is:

$$F_h = -kx \tag{8}$$

where k is the spring constant of each spring (N/m). To meet the per-leg normal force, the compressive force applied by each spring must be equal to or greater than the minimal required normal force to oppose friction, hence:

$$F_h \geq N_{\text{each}} \tag{9}$$

$$k\Delta x \geq \frac{mg}{n \cdot \mu_s} \tag{10}$$

Frictional Coefficient Assumptions: Dust build-up in HVAC ducts changes the effective friction at the wheel–surface interaction location. In clean conditions, friction arises largely from surface asperities interlocking and interfacial shear stresses. In dust conditions, when dust builds up in a loosely bonded, intermediate layer, dust does not contribute to mechanical interlocking mechanisms, and so acts as third-body particles and interrupts available resistance to slipping as a result of reduced mechanical interlocking in the bulk material.

For the reasons above, the highest friction coefficient was recorded at the lowest relative density of $\rho = 0.66$ with $d = 0.19$. As dust density increased, the surfaces became smoother, with d values leveling off at a constant of 0.13 beyond a relative density of $\rho = 0.8$. This reduction adversely affects traction and maneuverability, especially in the vertical or inclined portions of the duct system. However, no particular trends were visible in the measured static friction coefficients μ_s, while the mean static friction was $\mu_s = 0.23$, ranging from 0.19 to 0.29.

As with most experimental observations, exceptions exist. For example, under certain conditions dust can increase friction. This occurs when rough, asymmetric fragments under high load and humid conditions create a dense layer that is harder to displace compared to a looser setup.

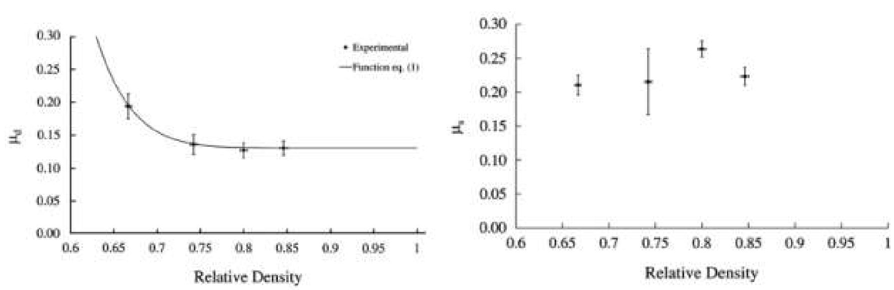

Fig. 2. predicted d and d values for relative dust densities

Results

Simulation Setup

The analysis process utilized *ANSYS* simulations to analyze two basic subsystems: the wheel-tire interaction, and the spring suspension system. The wheel simulated a single tire under load with the tire pressed against a vertical duct wall to review stress distribution on the upper tire surface; areas under high-cycle fatigue that lead to cracking, abrasion, and tearing were emphasized. The tire's reaction under static and dynamic compression was also analyzed in terms of flexibility and deformation. Mechanical parameters were defined to frame a representative simulation environment, including material stiffness, contact pressure on the tire disk, and friction coefficients. The suspension also used simulations to look at static and dynamic loading conditions, with static loading analyses able to define resting compression, and dynamic analyses able to define deformation, energy absorption, and recovery when operational forces are applied. The outcome of the tire and suspension subsystem simulation analysis enabled forecasting how variations in spring coefficients for suspension systems affect the stability being maintained as wall contact and traction are established during vertical climbs and when traversing uneven duct surfaces, such as during rapid movement.

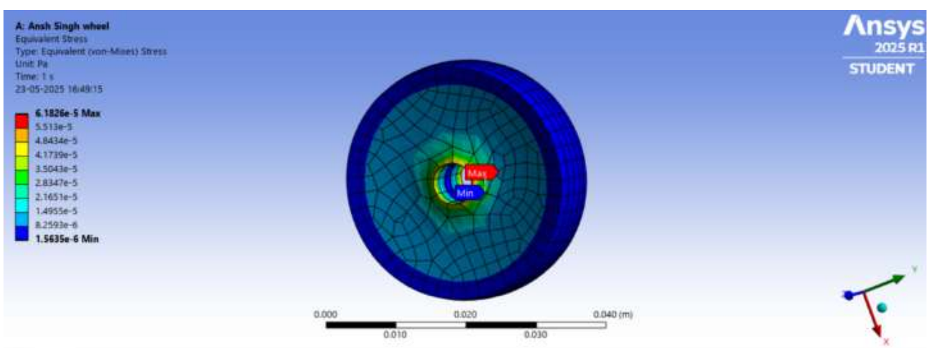

Fig. 3. simulation results of wheel under stress load conditions.

Loading Scenarios

In order to establish practical validity, three typical load cases were created:

1. **Static Suspension:** In this case, I allowed the robot to remain stationary and used solely the spring-driven normal forces for support. The question was to verify that the spring system would provide enough contact force to keep

the robot, when at rest, stable against gravity while still being compressed and deflected within an operationally safe amount.

2. **Vertical Motion Initiation:** This case modeled the beginning of either upward or downward motion. I wanted to evaluate whether or not the sum of spring compression and wheel–wall friction would be enough to avoid slippage and loss of traction during the initial acceleration or deceleration motion, which is usually the most critical in maintaining contact with the uneven duct walls.
3. **Dynamic Stability:** In this case, I assumed the robot was in a constant state of cleaning motion through the ducts. In the simulation, it was possible that the inertial forces caused by multiple rebounds of the springs and the usual cyclic vibrations of the cleaning motion, as well as impacts with duct junctions, and miscible transitions between surfaces could affect load distributions. The simulation results suggested that the system could work for cyclic loading while maintaining structural continuity and operational reliability. Continuing in a repetitive manner over an extended period of time allows the user to feel confident in the continual level of stability and continued cleaning regime.

Design Criteria (Max. and Min. Loads)

The design criteria were assessed by comparing the maximum compression of chosen spring coefficients (k), in N/m (spring constant), to the true minimum value of k needed in order to reach a maximum compression of 0.1 m. The results are summarized in Table 1.

Table 1. Calculated assumed k_{min} and actual k_{max} values for different loads.

Mass (kg)	**Weight (N)**	N_{each} **(N)**	**Spring coefficient** k **(N/m)**	**Max. Compression** Δx **(m)**	**Max.** Δx **(3 d.p)**	**Min.** k **for** $\Delta x = 0.1$**m**
5	49.05	12.2625	454.16	0.1500022019	0.150	681.25
5	49.05	12.2625	464.16	0.1467705102	0.147	681.25
5	49.05	12.2625	474.16	0.1436751308	0.144	681.25
8	78.48	19.62	726.60	0.1500137627	0.150	1090
8	78.48	19.62	736.60	0.1479771925	0.148	1090
8	78.48	19.62	746.60	0.1459951781	0.146	1090
10	98.10	24.525	908.30	0.1500055048	0.150	1362.5
10	98.10	24.525	918.30	0.1483719917	0.148	1362.5
10	98.10	24.525	928.30	0.1467736723	0.147	1362.5

The table presents a comparison between the calculated maximum compression values for assumed spring coefficients (k) in N/m and the actual minimum k required to achieve a maximum deflection of 0.1 m.

Stress Distribution Analysis

Simulated operational load shows that the wheel experiences torque loading of approximately 1.32×10^5 Pa of von Mises stress at the maximum peak value. There were significant stress concentrations primarily at the hub–shaft interface and at the root of the spokes. This redistribution of stress as primarily contour stresses became restricted to the wheel body and did not lead to uncontrolled deformations. The bounded strain was limited below the contour regions so that the geometry would be stable without inflection points due to stress concentration. Furthermore, the von Mises stress values remained well below the yield strengths of commonly used thermoplastics—ABS (4.4×10^7 Pa) and PLA (6.0×10^7 Pa). These results confirm the geometry selected and the material used for the given operating conditions. It is confirmed that the stresses were limited to the elastic region and that the loads were not sufficient to cause fractures or permanent deformation. As a result, the robotic's structure will able to complete repeated operational cycles in HVAC duct cleaning applications with no loss of long-term structural integrity or functional performance.

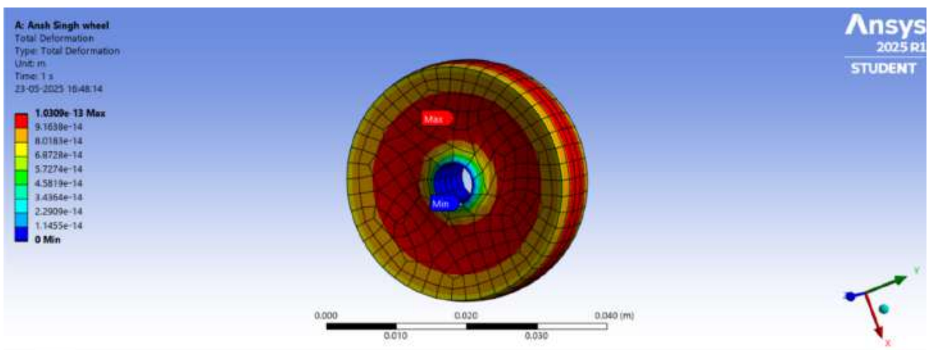

Fig. 4. simulation image of wheel deformation

Deformation Behaviour

In practical terms, the total deformation per unit load was computed using $m = 1.03 \times 10^{-13}$, which yields an output that is inconsequential. The simulation results indicated minute deflection, which suggests the wheel acts almost as a rigid body under the applied load. The rigidity allows for more effective transfer of torque with less energy loss. However, the minute deflection raises concern regarding the system's ability to absorb shocks and dampen vibrations when the robots pass laterally through gaps and joint spaces of a single duct or surface anomalies present in HVAC ducts.

The minute deformation can be explained through the overly constrained boundary conditions assumed in the simulation assuming high reversibility materials are used. While structuring for rigidity is advantageous for energy transfer, it also increases the transmission of external vibrations to the robot's frame. The external vibration may also affect sensitive on-board components, such sensors, and electronics. This warrants consideration during design to find a balance between the rigidity intended and transfer of external forces.

Safety Factor Distribution

The simulation results report a minimum factor of safety greater than 10, which shows that the applied stresses on the structural components remain far below the yield stress of the material. The factor of safety margin on structural reliability applies throughout the entire wheel geometry, including areas of noted stress concentration at the spoke-root junctions and shaft-bearing interfaces which would be of continuous concern during the design phase.

While a factor of safety this high confirms structural reliability, it also indicates potential overdesign. Larger structural components can not only take away available space within ducts, they can limit efficiency in terms of overall facilities energy turnover especially as the design objective in HVAC systems often target compact ducts. The constraints of vertical duct design facilitate an optimization for safe operational positioning, yet also identify potential optimization, whether through material reduction, lightweighting designs, etc., to facilitate both safe operation and balance safety with both efficiency and manoeuvrability.

Implications for Spring Constant Selection

The simulation-derived deformation value allows for theoretical estimation of the effective spring constant (k) of the wheel tire system, using Hooke's law:

$$k = \frac{F}{x} \tag{11}$$

Assuming a load of $F = 5$ N (based on robot weight and distribution), and a deformation of $x = 1.03 \times 10^{-13}$ m, the stiffness becomes:

$$k = \frac{5}{1.03 \times 10^{-13}} \approx 4.85 \times 10^{13} \text{ N/m} \tag{12}$$

This theoretical stiffness value is unrealistically high, indicating that the simulation does not incorporate compliant elements such as tire treads, rubber interfaces, or spring-damped mounting systems. In practical deployment, such excessive rigidity would lead to undesirable transmission of shocks, potential damage to the robot's frame, and a reduction in surface traction within ducts.

For effective duct navigation, where the wheel must adapt slightly to surface irregularities while maintaining sufficient normal force, a more practical spring constant range would fall between:

$$k = 500\text{–}3000 \text{ N/m} \tag{13}$$

This range allows about 0.5–2 mm of displacement under typical wheel loads (2.5–10 N) so it can get both compliance and structural support at an internal stiffness. These softer polymers, such as TPU or silicone-based treads, are able to achieve this target stiffness by way of micro-suspensions, flexural-elements, or both. Adaptive stiffness mechanisms such as magnetorheological materials, or variable-geometry flexures, may offer ways to dynamically adjust the stiffness based on changing terrain conditions or changes in duct curvature.

Comparative Implications and Future Design Optimization

The existing wheel configuration shows excellent safety and strength; but, the excessively rigid mechanical characteristics that are realized by absent deformation and extraordinarily high spring stiffness highlights a need for additional design improvement.

- Integrating compliant material zones in the tire cross-section
- Using suspension coupling at wheel–hub joints to decouple chassis and surface-induced vibrations
- Employing topology optimization to reduce material use while maintaining safety
- Considering biomimetic tread geometries for improved traction and damping

In addition, fatigue testing under cyclic loading, along with thermal stress simulations, should be conducted to assess long-term durability and material degradation, particularly for polymer-based wheels operating in thermally variable HVAC environments.

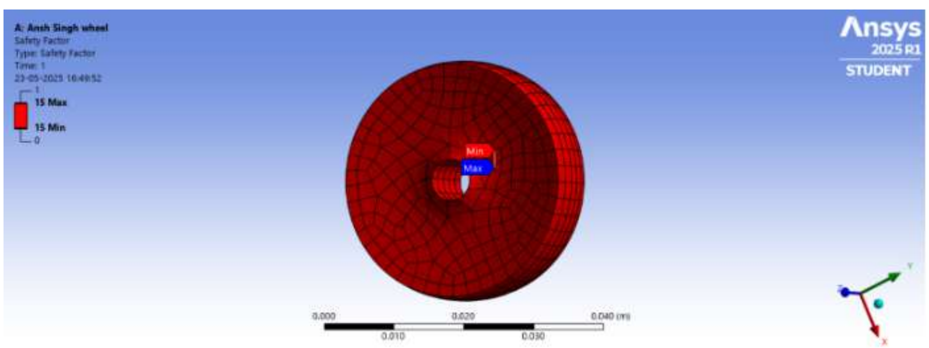

Fig. 5. simulation image of wheel safety factor

VII. CONCLUSION

This study tackles an important problem regarding the degradation of indoor air quality due to the accumulation of dust and pollutants in HVAC ducts by proposing a highly flexible and mobile robotic cleaning solution. The design uses aspects of traditional duct maintenance methods to get a broader picture, but overcome their limitations for accessing and cleaning duct components, safety concerns, and the lack of flexibility that often exists with duct shapes and geometries. The scissor mechanism is the key to the system, and allows for an adjustment to be made utilizing compressive forces with precise control for self-adjustment across different sizes of ducts and duct components. The proposed design is not confined to one set shape like traditional cleaning solutions that are suited specifically for one geometry, but can clean rectangular ducts, circular ducts of varying diameters, and other shapes.

The spring mechanisms were fundamental for two reasons: (1) providing a vertical mode; and (2) providing a uniform load to all contact points to provide and stick and traction to allow users to control the robot with the correct balance. Simulation results demonstrated that the wheels had structural integrity and were able to withstand the load in multiple arrangements. Using output from the simulations, Von Mises stresses were always below the yield strengths of each of the input materials use (PLA, ABS, TPU), providing mechanical assurance for successful use of the design in practice. Using the deformation presents that it acted as a rigid-body, by effectively contorting vibration, the internal safety factors that exceed 10 clearly shifted the performance to a unique, robust, resilient performance.

Overall, the spring-based pantograph mechanism is an example of the successful application of basic mechanical concepts in a practical and user-friendly robotic system. Future work may include expanding the system to include large HVAC networks, adding adaptive features for variable operational constraints, and increasing automation for use in real-world settings.

References

1. Y. Momma, et al., “Square Duct Cleaning Machine Using a Multistage Planetary Gear Mechanism for Removing Grease,” *IEEE Access*, 2024.
2. H. Yan, et al., “Study on Dynamic Characteristics of Pipeline Jet Cleaning Robot,” *Actuators*, vol. 13, no. 2, MDPI, 2024.
3. A. S. N. Husainy, et al., “Robotic Solutions for Air Duct Cleaning: An Overview of Current Research and Applications,” *Asian Review of Mechanical Engineering*, vol. 11, no. 2, pp. 27–31, 2022.
4. F. dos Santos Aureliano, A. F. Alves, and R. Franklin, “Eulerian Video Magnification for Cleaning and Inspection of Air Conditioning Ducts with Rover Robot.”
5. M. Bubanja, et al., “Robot for cleaning ventilation ducts,” in *New Technologies, Development and Application 4*, Springer International Publishing, 2019.
6. M. I. Seo, et al., “Control system design of duct cleaning robot capable of overcoming L and T-shaped ducts,” *IAES International Journal of Robotics and Automation*, vol. 9, no. 2, pp. 123, 2020.
7. Y. Tanise, et al., “Development of an air duct cleaning robot for housing based on peristaltic crawling motion,” in *Proc. 2017 IEEE International Conference on Advanced Intelligent Mechatronics (AIM)*, IEEE, 2017.

8. B. B. V. L. Deepak, M. V. A. R. Bahubalendruni, and B. B. Biswal, “Development of in-pipe robots for inspection and cleaning tasks: Survey, classification and comparison,” *International Journal of Intelligent Unmanned Systems*, vol. 4, no. 3, pp. 182–210, 2016.
9. A. Bulgakov and D. Sayfeddine, “Air conditioning ducts inspection and cleaning using telerobotics,” *Procedia Engineering*, vol. 164, pp. 121–126, 2016.
10. Z. Li, J. Zheng, and X. Lin, “Research on Biomimetic Robot-Crocodile Used for Cleaning Industrial Pipes,” in *International Conference on Computer Science and Information Engineering*, Springer, Berlin, Heidelberg, 2011.
11. C. Ye, et al., “Development of a pipe cleaning robot for air conditioning system,” in *Proc. 2010 IEEE International Conference on Robotics and Biomimetics*, IEEE, 2010.
12. M. Tavakoli, L. Marques, and A. T. de Almeida, “Development of an industrial pipeline inspection robot,” *Industrial Robot: An International Journal*, vol. 37, no. 3, pp. 309–322, 2010.
13. Y. Wang and J. Zhang, “Autonomous air duct cleaning robot system,” in *Proc. 2006 49th IEEE International Midwest Symposium on Circuits and Systems*, vol. 1, IEEE, 2006.
14. B. Tao, Z. Gong, and H. Ding, “Climbing robots for manufacturing,” *National Science Review*, vol. 10, no. 5, 2023, Art. no. nwad042.
15. H. Zhang, J. Zhang, and G. Zong, “Requirements of glass cleaning and development of climbing robot systems,” in *Proc. 2004 International Conference on Intelligent Mechatronics and Automation*, IEEE, 2004.